Downscaling algorithms for annual TRMM data based on climatic and orographic variables over the Qinling Mountains, China

Qing Meng[a]*, Ranjan Sarukkalige[b], Guobin Fu[c], Guan Wang[d], Wenhao Jia[e], Zhuang Liu[f], Hongying Bai[g], Xiaobang Peng[a], Shanhong Zhang[a]

[a] College of Urban, Rural Planning and Architectural Engineering, Shangluo University, Shangluo 726000, China

[b] Department of Civil Engineering, Curtin University, Western Australia, Australia

[c] CSIRO Land and Water, Private Bag 5, Wembley, WA 6913, Australia

[d] China South-to-North Water Diversion Eastern Route Corporation Limited, Beijing 100070, China

[e] Pearl River Water Resources Research Institute, Guangzhou 510611, China

[f] State key laboratory of Geo-information Engineering, Xi'an 710109, China

[g] Shaanxi Key Laboratory of Earth Surface System and Environmental Carrying Capacity, College of Urban and Environmental Science, Northwest University, Xi'an 710127, China

* Corresponding author at: College of Urban, Rural Planning and Architectural Engineering, Shangluo University, Shangluo 726000, China

E-mail address: qingmengmq@163.com

Abstract

Obtaining the gridded precipitation data with a high resolution in mountainous area is of importance in hydrology, meteorology, and ecology. However, rain gauge observations and satellite - based precipitation products have its own shortcomings. Precipitation in mountainous area has correlation with variables like elevation, slope, and temperature. In this study, we applied a downscaled algorithm called Geographically Weighted Regression (GWR) to obtain a fine resolution (1km) gridded precipitation data from the Tropical Rainfall Measuring Mission (TRMM) data at 0.25° resolution based on an assumption that precipitation in mountainous area has correlation with some orographic factors (elevation, slope, and aspect) and climatic factors (temperature, wind velocity, and humidity). The results indicated that (1) GWR improved the accuracy of TRMM data in the Qinling Mountains (r = 0.86, BIAS = - 2.77 %, and RMSE = 93.24 mm for annual downscaled precipitation during 2013 - 2015 periods, and r = 0.71, BIAS = - 3.60 %, and RMSE = 99.31 mm for annual TRMM data during 2013 - 2015 periods). (2) GWR showed a good performance in the southern part of the Qinling Mountains, while showed a worse performance in the northeast part of the Qinling Mountains. (3) Not only orographic factors but climatic factors were all essential in downscaling precipitation in mountainous areas. The more input factors, the more accurate downscaled result derived from GWR.

Keywords: precipitation; downscaling, GWR; TRMM; the Qinling Mountains

Introduction

As one of the crucial climatic factors, precipitation not only participates in water cycle for material and energy exchange, but also is the main source of surface fresh water and the basic material basis for crop growth. Precipitation may also induce drought and flood disasters and secondary geological disasters caused by it. Gridded precipitation data with a high spatial and temporal resolution is one of the initial inputs for hydrological models, climate prediction, and drought monitoring (Spracklen et al., 2012; Mou Leong TanVivien P et al., 2018). Point measurement could not reflect the actual temporal and spatial changes of precipitation in mountainous area because of instrumental limitations, sparse and uneven gauge distributions (Tang et al., 2018).

At present, spatial interpolation and satellite detection are effective ways to obtain gridded precipitation data. However, different interpolation methods could get different results, and usually the error is relatively large. With the advance in remote sensing technology, there are diverse range of satellite products, such as the Tropical Rainfall Measurement Mission (TRMM) Multi - satellite Precipitation Analysis (Huffman et al., 2007), the Climate Prediction Center (CPC) morphing technique (Joyce et al., 2004), Precipitation Estimation from Remotely Sensed Information using Artificial Neural Network (Sorooshian et al., 2000). TRMM have been widely used with a better performance which is favored for the development of the methodology as it is an operational product (Dinku et al., 2007; Li and Shao, 2010; Gefei et al., 2017; Hunink et al., 2014; Chen et al., 2018; Yueyuan et al., 2018; Ma et al., 2017; Jian et al., 2013). The accuracy of TRMM data is in good agreement with the measured stations at low altitudes, especially at high altitudes is uncertain (Stampoulis and Anagnostou, 2012; Tian and Peters - Lidard, 2010). Although these current satellite precipitation products span a wide range, the resolution is relatively coarse. This makes to acquire the accurate precipitation grid data with a high temporal and spatial resolution a key challenge currently, especially in data - lacking mountainous area, which has a complicated terrain condition. In addition, satellite - based precipitation datasets contain inherent uncertainty derived from retrieval algorithms, topographic errors, and clouds (Adhikary et al., 2015; Chen, 2013).

Precipitation changes in mountainous areas are often related to topography, slope, aspect and other micro - topographical characteristics, which can deform the wind fluxes and perturbation and make accuracy of satellite precipitation products not guaranteed (Wang and Georgakakos, 2003). Terrain conditions are also considered to be a significant factor in correcting precipitation accuracy in many studies (Shaofeng et al., 2011; Duan and Bastiaanssen, 2013). Theoretically, the higher elevation, the more humid of air masses, result in precipitation. Also, aspect could alter the direction of airflow, thus determining the excess or deficit of precipitation. As for slope, a gradient of vertical airflow may control the intensity and area of precipitation (Badas et al., 2005). Therefore, it is necessary and urgent to downscale satellite precipitation products in mountainous areas considering orographic factors. Jian et al. (2013) downscale precipitation based on the correlations between observed precipitation and orographic factors, such as slope, aspect and terrain roughness, as well as humidity and temperature. Shaofeng et al. (2011) improved downscaling result by adding elevation data. Meanwhile, a lot of efforts have been made to obtain high resolution grid precipitation data (Lu et al., 2019; Xu et al., 2015). Immerzeel et al. (2009) corrected the satellite precipitation product by adding normalized difference vegetation index (NDVI). Different statistical methods could be applied to downscale satellite precipitation products to a high resolution and get better correction results. Duan and Bastiaanssen (2013) adopted geographical differential analysis (GDA) and geographical ratio analysis (GRA) to generate a monthly TRMM data at 1 km resolution. Geographically weighted regression (GWR) was proposed by Xu et al. (2015) and Lu et al. (2019) to downscale the satellite precipitation data over the Tianshan Mountains, and results showed GWR method outperformed other statistical methods. Quadratic parabolic profile (QPP) model for downscaling TRMM data was introduced by Yueyuan (2018), which had higher accuracies than other commonly used methods. Ma et al. (2017) implemented a spatial data mining algorithm called Cubist to downscale the TRMM data from 0.25° to 1 km resolution over the Qinghai - Tibet Plateau. Although prior researches were based on vegetation and terrain factors when downscaling, some scholars pointed out that other factors such as land use and temperature could also affect precipitation when downscaling the satellite data (Chen et al. 2015; Immerzeel et al., 2009; Shaofeng et al., 2011; Foody, 2003; Yang G et al., 2012).

Although there are many downscaling methods to obtain a specific and higher resolution precipitation data based on different satellite sources of data, challenges also exist in downscaling in mountainous areas due to lack of observations and with complicated terrain and variation in precipitation. As a transitional zone in China, it is the geographical boundary of south China and north China, sub - humid and sub - dry regions, warm and sub - tropical regions, it's also famous for large altitude difference, with a peak altitude is as high as 3771.2 m. In this study, we applied geographically weighted regression (GWR) which was designed to deal with spatial heterogeneity and widely used in downscaling satellite precipitation product (Brunsdon et al,. 1996; Xu et al., 2015; Chen et al., 2018.) to downscale the TRMM 3B43 V7 data from 0.25° to 1 km resolution considering the impacts of topographical and climatic factors on precipitation. NDVI was omitted in our study as some studies showed that the effect of vegetation on precipitation has time lag about 2 - 3 months (Immerzeel et al., 2005; Heidinger et al., 2012). The specific aims of this study are to downscale satellite precipitation into a higher resolution (1km) using GWR method, considering not only topographic factors like elevation, slope and aspect but climatic factors like temperature, humidity and wind velocity.

1. Study area and data

1.1 Study area

The Qinling Mountains (32°54′ - 34°35′N, 105°30′ - 111°3′E) occupies the southern part of Shaanxi Province in central China. Carrying a total area of 61,900 km^2 (Fig. 1). The elevation of the Qinling Mountains ranges from 195 m to 3771.2 m. It stretches as far as 400 - 500 km from east to west and 120 - 180 km from south to north. As a transitional zone in China, it is the geographical boundary of south China and north China, sub - humid and sub - dry regions, warm and sub - tropical regions. The south region receives the highest annual precipitation of 1156 mm, while the northern region receives 545 mm average precipitation annually. The average annual precipitation is approximately 825 mm. More than 70% of the annual precipitation observed from May to September in the Qinling Mountains, and more precipitation is detected in the south and less in the north (Shaozhuang et al., 2018)

1.2 Data

1.2.1 TRMM dataset

TRMM is a joint project of the National Aeronautics and Space Administration (NASA) and Japan Aerospace Exploration Agency (JAXA) launched on 27 November 1997, with the aim of monitoring and studying rainfall in tropical and subtropical regions between 50° N and 50°S globally (Kummerow et al., 1998). TRMM carries several precipitation measuring instruments, including the Precipitation Radar (PR), the TRMM Microwave Imager (TMI) and the Visible & Infrared Scanner (VIRS). Several algorithms have been developed to retrieve precipitation using information from these instruments and has provided valuable information on rainfall and easy to obtain (Haddad, 1997; Iguchi et al., 2016; Huffman et al., 2007). The Tropical Rainfall Measuring Mission (TRMM) 3B43 Version 7 with a resolution of 0.25° is a standard monthly precipitation dataset from 2013 to 2015 and was obtained from NASA.

1.2.2 Digital Elevation Model data (DEM)

The DEM used in this study was collected from Shaanxi Bureau of Surveying, Mapping and Geoinformation at 25 m spatial resolution. For further study, it was resampled to 1 km by Bi - linear method. Other input layers of the model like slope (Slo) and aspect (Asp) were all derived from DEM, and these orographic variables were transformed into the same resolution of 1 km.

1.2.3 In situ meteorological data

Monthly precipitation data (Pre), humidity data (Hum), temperature data (Tem) and wind velocity (Win) data from December to February of 32 meteorological stations from 2013 to 2015 used in this study. In order to prepare for the next step, all these climatic data were interpolated by Ordinary Kriging method and resampled into the same spatial resolution of 1 km by Bi - linear method.

2. Methodology

2.1 Geographical Weighted Regression (GWR)

GWR is a regression method that can be used to solve location - related issues on Tobler's first law of geography that is "everything is related to everything else, but near things are more related than distant things". In this study, we use GWR 4.0 software to run GWR model. The model is established by generating parameters for the independent variable and explanatory variable of each given cell. The following equation can express the GWR:

$$Y_j = \beta_0\left(u_j, v_j\right) + \sum_{k=1}^{p} \beta_k\left(u_j, v_j\right) X_{kj} + \varepsilon_j \qquad (1)$$

where Y_j represent the dependent variable observations precipitation, X_{kj} represent the *kth* independent variable. β_0 (u_j, y_j) and β_k (u_j, y_j) denote the intercept and slope estimated at the *j*th point. Parameter ε_j denotes the residual of this model. The coefficients in Eq. (1) are estimated from the neighboring observations of the point *j*, with a weighted function based on an assumption that the closer observations are to point *j*, the more influenced weight by the point *j*. The coefficients can be calculated by the following Eq. (2)

$$\hat{\beta}(u_j, v_j) = \left(X^T W(u_j, v_j) X\right)^{-1} \left(X^T W(u_j, v_j) P\right) \tag{2}$$

where $\hat{\beta}(u_j, v_j)$ represents the local coefficient estimated at point *j*, *X* and *P* represents the independent and dependent variables, respectively. $W(u_j, v_j)$ is the weight matrix. In this study, this weight value can be express by the following Eq. (3)

$$\begin{aligned} w_{ij} &= \left[1-\left(d_{ij}/b\right)^2\right]^2 \text{ when } d_{ij} \le b \\ w_{ij} &= 0 \text{ when } d_{ij} > b \end{aligned} \tag{3}$$

where d_{ij} is the distance between point *j* and the neighboring observation *i*. *b* is the bandwith threshold.

2.2 Main steps of downscaling algorithm

(1) Interpolated all the in situ observations layers by Ordinary Kriging method. Resampled TRMM data, precipitation observations and all climatic (temperature, humidity, wind velocity) and orographic (elevation, slope, aspect) factors into the same resolution of 1 km by Bi - linear method, and then converted them into a point data from the raster format to enable extraction of values from every layer at the same location. These 8 layers were all set the projection coordinate system. The flowchart of downscaling algorithm of GWR in this study was shown in Fig. 2.

(2) Treated TRMM data, climatic (temperature, humidity, wind velocity) and

orographic (elevation, slope, aspect) factors as independent variables, precipitation observations as dependent variable. To study which factors could better simulated the TRMM data, we experimented 6 models which consider different factors in GWR as shown in Table 1.

(3) In GWR, two parameters are critical: the kernel function and the selection criteria. There are four kernel functions (Fixed Gaussian, Fixed bi - square, Adaptive bi - square and Adaptive Gaussian) and four selection criteria (Akaike information criterion (AIC), small sample bias corrected (AICc), Bayesian information criterion (BIC), and cross validation (CV)). Adaptive could produce more concrete result than Fixed method, that is why Adaptive bi - square and Adaptive Gaussian were chosen as the Kernel type in this study, respectively. Selection Criteria of CV designed only match for Gaussian. So, we tested four kinds of Kernel type and Selection Criteria in this study. Eventually, Adaptive bi - square and AICc was tested to get the best estimations and we use these two indices in GWR.

2.3 Validation

The following three validation indices were chosen to compare the accuracy of downscaling model in this study. They are Pearson correlation coefficient (r), root mean square error (RMSE), and relative bias (Bias). These indicators are calculated by Eqs. as follows, respectively:

$$\mathrm{r} = \frac{\sum_{i=1}^{n}\left(x_i - \overline{x}\right)\left(y_i - \overline{y}\right)}{\sqrt{\sum_{i=1}^{n}\left(x_i - \overline{x}\right)^2 \sum_{i=1}^{n}\left(y_i - \overline{y}\right)^2}} \qquad (4)$$

$$\text{RMSE}=\sqrt{\frac{\sum_{i=1}^{n}\left(x_i-y_i\right)^2}{\text{n}}} \tag{5}$$

$$BIAS=\frac{\sum_{i=1}^{n}\left(x_i-y_i\right)}{\sum_{i=1}^{n}y_i}\times 100\% \tag{6}$$

where x and y represent the original precipitation and estimated precipitation, respectively. They were calculated based on the original precipitation values and estimated precipitation values to evaluate the GWR method. When r is approaching 1 representing the relationship is better. An RMSE and BIAS approximately 0 representing the estimated value approach the original value.

3. Results and Discussion

3.1 Spatial distribution of original and downscaled precipitation

The observed annual mean precipitation and annual TRMM 3B43 data during 2013 - 2015 periods in the Qinling Mountains are compared to check the variations. As shown in Fig. 3, original TRMM 3B43 apparently overestimated the observation precipitation (OBS) in 2014 and 2015, but underestimated in 2013. Hence, we compared the downscaled annual precipitation in the Qinling Mountains during 2013 - 2015 periods with observation and TRMM data.

The spatial patterns of precipitation obtained from original TRMM data, observed precipitation, and downscaled precipitation by GWR in the Qingling Mountains from 2013 - 2015 periods are showed in Fig. 4. The spatial patterns are basically the same for all three sources. Precipitation ranged 350 to 1200 mm and high precipitation occurred at the southern part of the Qinling Mountains, while the northern part of the Qinling Mountains received low precipitation. Otherwise, we could see that downscaled precipitation were more smoothly than other two precipitation data. Comparing with other two precipitation results from Fig. 4 downscaled precipitation avoided "Bull Eye" phenomenon because of considered orographic and climatic factors. Thus, it had less error with original precipitation.

Fig. 5 showed the spatial distribution of evaluation indices between original TRMM data and downscaled precipitation over the Qinling Mountains. Original TRMM data showed a good performance in the western part of the Qinling Mountains. In contrast, downscaled results showed a better performance in the southern part the Qinling Mountains, but showed a worse performance in the northeast part.

3.2 Validation

Table 2 shows the maximum, minimum, and mean precipitation of TRMM, OBS, and GWR. It could be found that maximum, minimum, and mean precipitation of GWR were closer to the observed data in every year compared with TRMM data; TRMM maximum precipitation in 2014 was 1020.74 mm, OBS and GWR were 947.85 mm and 931.81 mm, respectively. Overall, GWR introduced orographic and climatic factors influencing precipitation could improve the overestimated precipitation detected by TRMM.

For evaluating the effect of downscaling algorithm quantitatively, three evaluation indices of TRMM and GWR from 2013 to 2015 periods in the Qinling Mountains are shown in Table 3. It could found that GWR has improved the TRMM data; Pearson correlation coefficient (r) has increased from 0.71 to 0.86; relative bias

(Bias) reduced from - 3.60 to - 2.77; RMSE also decreased from 99.31 to 93.24.

Scatter plots in Fig. 6 depicted the TRMM and GWR model against the OBS in 2013, 2014, and 2015. GWR were the closest to 1:1 line, and TRMM data were the most dispersed distribution during these three years, which also reflected precipitation accuracy can be simulated more accurately by GWR downscaled model. GWR improved r from 0.89 to 0.94 in 2013, especially in 2014 and 2015, GWR were more correlated with observed precipitation than TRMM, with r from 0.56 to 0.77, and from 0.67 to 0.87, respectively.

Many geostatistical techniques were used to downscale precipitation in mountainous areas. For example, Regression Kriging has been found useful for downscaling low resolution precipitation datasets (Zhang et al., 2018) for its advantage to extend to a border range of regression techniques and allow separate interpolation of the two interpolated components (Hengl et al., 2007). The satellite precipitation datasets were predicted using global regression, which had not thoroughly considered the relationship between precipitation and environmental variables were spatially varying and scale-dependent (Xu et al., 2015). GWR has the advantage of investigating the non-stationary and scale-dependent characteristics of the relationship between the variables (Xu et al., 2015; Foody, 2003) and is suitable for detecting complex relationships between precipitation and other environmental variables (Chen et al., 2014). In the future, some new techniques like artificial intelligence machine learning, and data mining could be applied in this field.

3.3 Performances of different GWR models

For detecting which influencing factor is the most important when downscaling annual precipitation in the Qinling mountainous area, we designed different downscaling models considering different influencing factors as shown in Table 1. Model 1 to model 3 considered orographic (elevation, slope, aspect) factors, and model 4 to model 6 considered climatic (temperature, humidity, wind velocity) factors, separately. Fig. 7 depicted the bar plot of downscaled precipitation and TRMM during 2013 - 2015 periods and Table 4 showed the comparison between different models of GWR from 2013 to 2015 periods in the Qinling Mountains. From model 1 to model 6, the *r* is 0.85, 0.85, 0.85, 0.85, 0.86, 0.86, respectively, indicating that these 6 models have strong linear correlation with the observed precipitation. The BIAS from model 1 to model 6 were - 3.23, - 3.27, - 3.27, - 3.15, - 2.93, - 2.77, respectively, and the RMSE were 94.05, 93.97, 93.84, 93.78, 93.41, 93.24, respectively, which all indicating that model 6 which considered all the orographic and climatic factors showed the best performance, with the highest r (0.86), lowest RMSE (- 2.77) and BIAS (93.24). This result explained the downscaled algorithm which considered all the orographic and climatic factors could get the best downscaling performance, indicating that these factors all are well - related to precipitation in mountainous area.

Fig. 8 showed the Taylor diagrams of different downscaled models with observed and TRMM data. Taylor diagram can show the correlation coefficient, standard deviation (SD) and RMSE in the same figure. The closer the point of downscaled precipitation to the point of observed precipitation, the better the accuracy of the downscaled precipitation. Fig. 8 all showed point H (Model 6) is the closet to the point A (Observed precipitation). Especially in 2014, the SD of observed precipitation was 89.96mm, while the SD of model 6 was 77.32 mm. The model 6 was 0.77, and the RMSE was the lowest.

NDVI was designed as a vital element in downscaling precipitation for its responses in past research (Wang et al., 2001; Barbosa and Kumar, 2016; Immerzeel et al., 2009; Wenlong et al., 2016; Duan et al., 2013), but some scholars pointed out that there is at least three month of lag time between vegetation and precipitation. Furthermore, a higher NDVI does not represent heavy precipitation in humid zone because of saturated NDVI (Shi and Song, 2015; Shi et al., 2015). In some cases, different land use could change the NDVI, such as water, snow, and barren. Thus, we should detect these NDVI anomalies and eliminate during data processing in the future. Generally, vegetation was nourished by precipitation. Thus, introducing NDVI in downscaling precipitation need to be further studied.

The orographic effect is regarded as a vital aspect in shaping precipitation in mountainous areas. Lot of researchers have studied orographic effect in downscaling precipitation (Jia et al., 2011; Guan et al., 2009; Badas et al., 2005; Reid, 1973; Smith, 1979). Furthermore, the temp - spatial variation of precipitation is influenced by other land factors. For example, Schultz and Halpert (1995) found that incorporated land surface temperature with the NDVI in projecting precipitation, the accuracy is more precise when compared with using NDVI alone at a global scale. Many scholars implemented better downscaled precipitation results after incorporated temperature factor (Jing et al., 2016; Ma et al., 2017). Thus, we not only incorporated elevation, aspect, and slope, but also temperature, wind velocity, and humidity into the downscaled scheme in our study.

3.4 Precipitation variations in the Qinling Mountains of 14 years based on GWR

From the above research, it can be seen that the precipitation grid data obtained on the annual scale of the Qinling Mountains based on the geographical weighted regression method has a certain degree of reliability. Therefore, the long - term precipitation data from 2002 to 2015 are verified and applied. The results are shown in Fig. 9. From the figure, it can be seen that the average annual precipitation in the Qinling Mountains over the past 14 years has ranged from 565.6 to 872.6 mm, with an average precipitation of 759.7 mm. The average precipitation in spring, summer, autumn, and winter in the Qinling Mountains from 2002 to 2015 was 113.6 to 236.4 mm, 233.5 to 433.2 mm, 123.7 to 275.7 mm, and 11.9 to 36.2 mm. The average precipitation in four seasons is in the order of summer (366.1 mm), autumn (221.8 mm), spring (146.4 mm), and winter (25.3 mm). Fig. 10 shows the distribution map of monthly average precipitation in the Qinling Mountains over the past 14 years. From the figure, it can be seen that July has the most precipitation in the Qinling Mountains, with a precipitation of 88.7 ~ 180.6 mm and an average precipitation of 141.9 mm, especially in the southern slope area.

In order to further test the scientificity and accuracy of the precipitation grid data of the Qinling Mountains over the past 14 years, the results are hereby verified. The results are shown in Tables 5 and 6. From the table, it can be seen that the precipitation grid data set of the Qinling Mountains from 2002 to 2015 is relatively close to the measured meteorological station data with high accuracy, indicating that its grid data set has high reliability and can be used as input parameters for hydrological and ecological models.

4. Conclusions

In this study, combined with rain gauge observations and satellite - based precipitation product, using orographic factors (elevation, slope, and aspect) and climatic factors (temperature, wind velocity, and humidity), a gridded precipitation with a 1 km resolution in mountainous area was downscaled by means of GWR at an annual scale. The main conclusions are as follows:

(1) The spatial distribution of original TRMM data, rain gauge observation, and downscaled precipitation were totally the same in the Qinling Mountains. Precipitation ranged from 350 mm to 1200 mm and high values all occurred at the southern part of the Qinling Mountains, while low values located at the northern part of the Qinling Mountains. TRMM data showed a good performance in the western part of the Qinling Mountains. GWR showed a better performance in the southern part of this area, while showed a worse performance in the northeast part of this area.

(2) Downscaled precipitation improved the accuracy of original TRMM data obviously at annually scale from 2013 to 2015 periods in the Qinling Mountains. It increased r from 0.71 to 0.86, and decreased BIAS from - 3.60% to - 2.77%, and decreased RMSE from 99.24 mm to 93.24 mm.

(3) 6 GWR models were developed, considering 6 different orographic and climatic factors. The more factors input, the more accurate the downscaled result

derived. Precipitation in mountainous area is related with not only orographic factors (elevation, slope, and aspect) but climatic factors (temperature, wind velocity, and humidity).

Acknowledgments: We would also like to thank Prof. Christian Bernhofer (Editor) and the anonymous reviewers for their invaluable comments and constructive suggestions used to improve the quality of the manuscript. The meteorological data were provided by Shaanxi Meteorological Bureau. The Tropical Rainfall Measuring Mission (TRMM) 3B43 Version 7 with a resolution of 0.25° is a standard monthly precipitation dataset from 2013 to 2015 and was obtained from NASA (https://mirador.gsfc.nasa.gov/cgi-bin/mirador/presentNavigation.pl?project=TRMM&tree=project).

Funding: This study was funded by the China Scholarship Council (CSC).

Conflicts of interest/Competing interests: There is no conflict of interest.

Author Contributions: Qing Meng and Guan Wang contributed to the study conception and design. Material preparation, data collection and analysis were performed by Qing Meng and Hongying Bai. The first draft of the manuscript was written by Qing Meng and all authors commented on previous versions of the manuscript. All authors read and approved the final manuscript.

Data Availability: The datasets generated and analyzed during the current study are not publicly available due to privacy and restrictions.

References

Adhikary S K, Yilmaz A G, Muttil N. Optimal design of rain gauge network in the Middle Yarra River catchment, Australia[J]. Hydrological Processes, 2015, 29, 2582–2599.

Badas M G, Deidda R, Piga E. Rainfall downscaling in montainous regions[J]. Geophysical Research Abstract, 2005, 7, 08974.

Barbosa H A, Kumar T. Influence of rainfall variability on the vegetation dynamics over Northeastern Brazil[J]. Journal of Arid Environments, 2016, 124(JAN.):377-387.

Brunsdon C, Fotheringham A S, Charlton M E. Geographically Weighted Regression: A Method for Exploring Spatial Nonstationarity[J]. Geograpgical Analysis, 1996, 28 (4),281–298.

Chen F, Yu L, Qiang L, et al. Spatial downscaling of TRMM 3B43 precipitation considering spatial heterogeneity[J]. International Journal of Remote Sensing, 2014, 35(9-10):3074-3093.

Chen Y. Evaluation of TRMM 3B42 daily precipitation estimates of tropical cyclones rainfall over the Pacific and Australia region[C]. 2013, 2184–2196.

Chena Y, Huanga J, Shengd S, et al. A new downscaling-integration framework for high-resolution monthly precipitation estimates: Combining rain gauge observations, satellite-derived precipitation data and geographical ancillary data[J]. Remote Sensing of Environment, 2018, 214:154-172.

Dinku T, Ceccato P E. Groverkgopec, et al. Validation of satellite rainfall products over East Africa's complex topography[J]. International Journal of Remote Sensing, 2007, 28(7):1503-1526.

Duan Z, Bastiaanssen W. First results from Version 7 TRMM 3B43 precipitation product in combination with a new downscaling–calibration procedure[J]. Remote Sensing of Environment, 2013, 131:1-13.

Foody G M. Geographical weighting as a further refinement to regression modelling: An example focused on the NDVI−rainfall relationship[J]. Remote Sensing of Environment, 2003, 88(3):283-293.

Gefei W, Peiyun Z, Liwen L, et al. Evaluation of precipitation from CMORPH, GPCP-2, TRMM 3B43, GPCC, and ITPCAS with ground-based measurements in the Qinling-Daba Mountains, China[J]. Plos One, 2017, 12(10):e0185147.

Guan H, Wilson J L, Xie H. A cluster-optimizing regression-based approach for precipitation spatial downscaling in mountainous terrain[J]. Journal of Hydrology, 2009, 375(3-4):578-588.

Haddad Z S. The TRMM 'Day-1' Radar/Radiometer Combined Rain-Profiling Algorithm[J]. Journal of the Meteorological Society of Japan, 1997, 75(4):799-809.

Heidinger H, Yarlequé, Christian, Posadas A, et al. TRMM rainfall correction over the Andean Plateau using wavelet multi-resolution analysis[J]. International Journal of Remote Sensing, 2012, 33(14):4583-4602.

Hengl T, Heuvelink G, Rossiter D G. About regression-kriging: From equations to case studies[J]. Computers & Geosciences, 2007, 33(10):1301-1315.

Huffman G J, Adler R F, Bolvin D T, et al. The TRMM Multisatellite Precipitation Analysis (TMPA): Quasi-Global, Multiyear, Combined-Sensor Precipitation

Estimates at Fine Scales[J]. Journal of Hydrometeorology, 2007, 8(1):38–55.

Hunink J E, Immerzeel W W, Droogers P. A High-resolution Precipitation 2-step mapping Procedure (HiP2P): Development and application to a tropical mountainous area[J]. Remote Sensing of Environment, 2014, 140:179-188.

Iguchi T, Kozu T, Meneghini R, et al. Rain-Profiling Algorithm for the TRMM Precipitation Radar[C]// Geoscience and Remote Sensing, 1997. IGARSS '97. Remote Sensing - A Scientific Vision for Sustainable Development. 1997 IEEE International. IEEE, 2016.

Immerzeel W W, Quiroz R A, De Jong S M. Understanding precipitation patterns and land use interaction in Tibet using harmonic analysis of SPOT VGT-S10 NDVI time series[J]. International Journal of Remote Sensing, 2005, 26(11):2281-2296.

Immerzeel W W, Rutten M M, Droogers P. Spatial downscaling of TRMM precipitation using vegetative response on the Iberian Peninsula[J]. Remote Sensing of Environment, 2009, 113(2):362-370.

Jian F, Du J, Wei X, et al. Spatial downscaling of TRMM precipitation data based on the orographical effect and meteorological conditions in a mountainous area[J]. Advances in Water Resources, 2013, 61(nov.):42-50.

Joyce R J, Janowiak J E, Arkin P A, et al. CMORPH: A Method that Produces Global Precipitation Estimates from Passive Microwave and Infrared Data at High Spatial and Temporal Resolution[J]. Journal of Hydrometeorology, 2004, 5(3):287-296.

Kummerow C, Barnes W, Kozu T, et al. The tropical rainfall measuring mission (TRMM) sensor package[J]. Journal of Atmospheric and Oceanic Technology, 1998, 15(3):809-817.

Li M, Shao Q. An improved statistical approach to merge satellite rainfall estimates and raingauge data[J]. Journal of Hydrology, 2010, 385(1-4): 51–64.

Lu X, Tang G, Wang X, et al. Correcting GPM IMERG precipitation data over the Tianshan Mountains in China[J]. Journal of Hydrology, 2019, 575: 1239–1252.

Ma Z, Shi Z, Zhou Y, et al. A spatial data mining algorithm for downscaling TMPA 3B43 V7 data over the Qinghai–Tibet Plateau with the effects of systematic anomalies removed[J]. Remote Sensing of Environment, 2017, 200: 378–395.

Mou Leong TanVivien P. ChuaKok Chooi TanK. Brindha. Evaluation of TMPA 3B43 and NCEP-CFSR precipitation products in drought monitoring over Singapore[J]. International Journal of Remote Sensing, 2018, 39(8), 2089–2104.

Reid I. The influence of slope aspect on precipitation receipt. Weather, 1973, 28, 490–494.

Schultz P A, Halpert M S. Global analysis of the relationships among a vegetation index, precipitation and land surface temperature[J]. International Journal of Remote Sensing, 1995, 16(15):2755-2777.

Shaofeng Jia, and, et al. A statistical spatial downscaling algorithm of TRMM precipitation based on NDVI and DEM in the Qaidam Basin of China[J]. Remote Sensing of Environment, 2011, 115, 3069–3079.

Shaozhuang G, et al. Landscape pattern change and its response to anthropogenic disturbance in the Qinling Mountains during 1980 to 2015.[J]. Ying yong sheng tai xue bao = The journal of applied ecology, 2018, 29(12):4080-4088.

Shi Y, Song L, Xia Z, et al. Mapping Annual Precipitation across Mainland China in the Period 2001−2010 from TRMM3B43 Product Using Spatial Downscaling Approach[J]. Remote Sensing, 2015, 7(5):5849-5878.

Smith R B. The Influence of Mountains on the Atmosphere[J]. Advances in Geophysics, 1979, 21:87-230.

Sorooshian S, Hsu K L, Gao X, et al. Evaluation of PERSIANN system satellite-based estimates of tropical rainfall[J]. Bull.amer.meteor.soc, 2000, 81(9), 2035–2046.

Spracklen D V, Arnold S R, Taylor C M. Observations of increased tropical rainfall preceded by air passage over forests[J]. Nature, 2012, 489(7415):282-285.

Stampoulis D, Anagnostou E N. Evaluation of Global Satellite Rainfall Products over Continental Europe[J]. Journal of Hydrometeorology, 2012, 13(2):588-603.

Tang G, Behrangi A, Long D, et al. Accounting for spatiotemporal errors of gauges: A critical step to evaluate gridded precipitation products[J]. Journal of Hydrology, 2018, 559, 294-306.

Tian Y, CD Peters□Lidard. A global map of uncertainties in satellite□based precipitation measurements[J]. Geophysical Research Letters, 2010, 37(24).

Wang J, Georgakakos K P. Validation and Sensitivities of Dynamic Precipitation Simulation for Winter Events Over the Folsom Lake Watershed: 1964-99[J]. Monthly Weather Review, 2003, 133(1):3-19.

Wang J, Price K P, Rich P M. Spatial patterns of NDVI in response to precipitation and temperature in the central Great Plains[J]. International Journal of Remote

Sensing, 2001, 22(18):3827-3844.

Wenlong J, Yaping Y, Xiafang Y, et al. A Comparison of Different Regression Algorithms for Downscaling Monthly Satellite-Based Precipitation over North China[J]. Remote Sensing, 2016, 8(10):1-17.

Xu S, Wu C, Wang L, et al. A new satellite-based monthly precipitation downscaling algorithm with non-stationary relationship between precipitation and land surface characteristics[J]. Remote Sensing of Environment, 2015, 162:119-140.

Yang G, Jiao H, Shuang L, et al. Spatial pattern of non-stationarity and scale-dependent relationships between NDVI and climatic factors—A case study in Qinghai-Tibet Plateau, China[J]. Ecological Indicators, 2012, 20:170-176.

Yueyuan Z, Yungang L, Xuan J, et al. Fine-Resolution Precipitation Mapping in a Mountainous Watershed: Geostatistical Downscaling of TRMM Products Based on Environmental Variables[J]. Remote Sensing, 2018, 10(1):119.

Zhang T, Li B, Yuan Y, et al. Spatial downscaling of TRMM precipitation data considering the impacts of macro-geographical factors and local elevation in the Three-River Check for updates Headwaters Region[J]. Remote Sensing of Environment: An Interdisciplinary Journal, 2018(215):109–127.

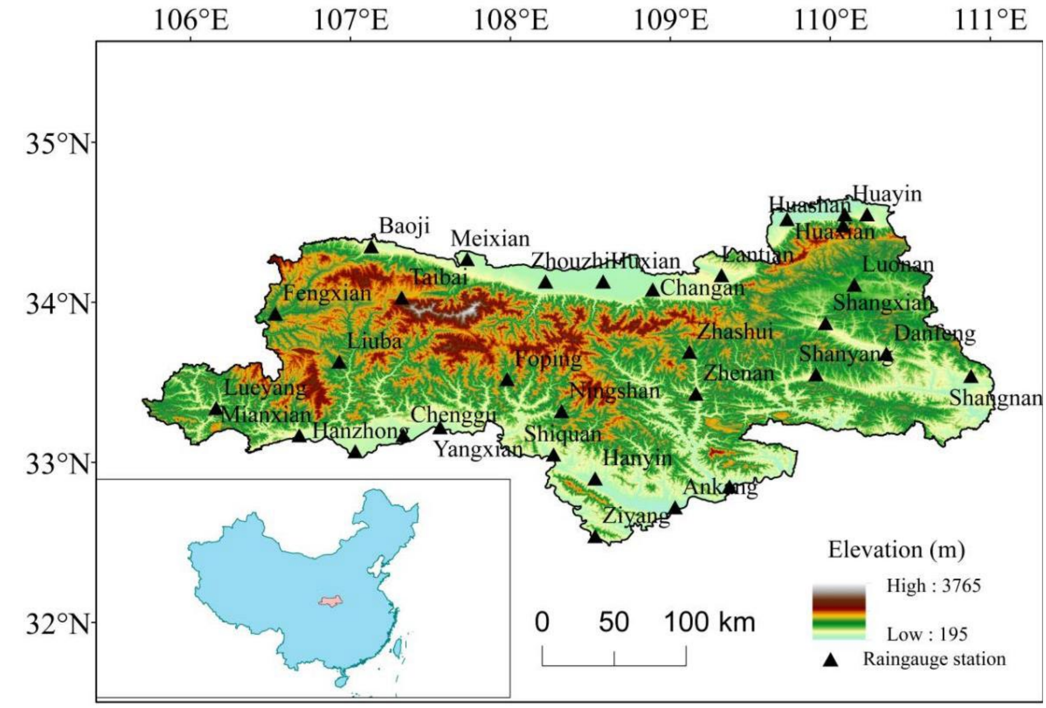

Fig.1 Study Area

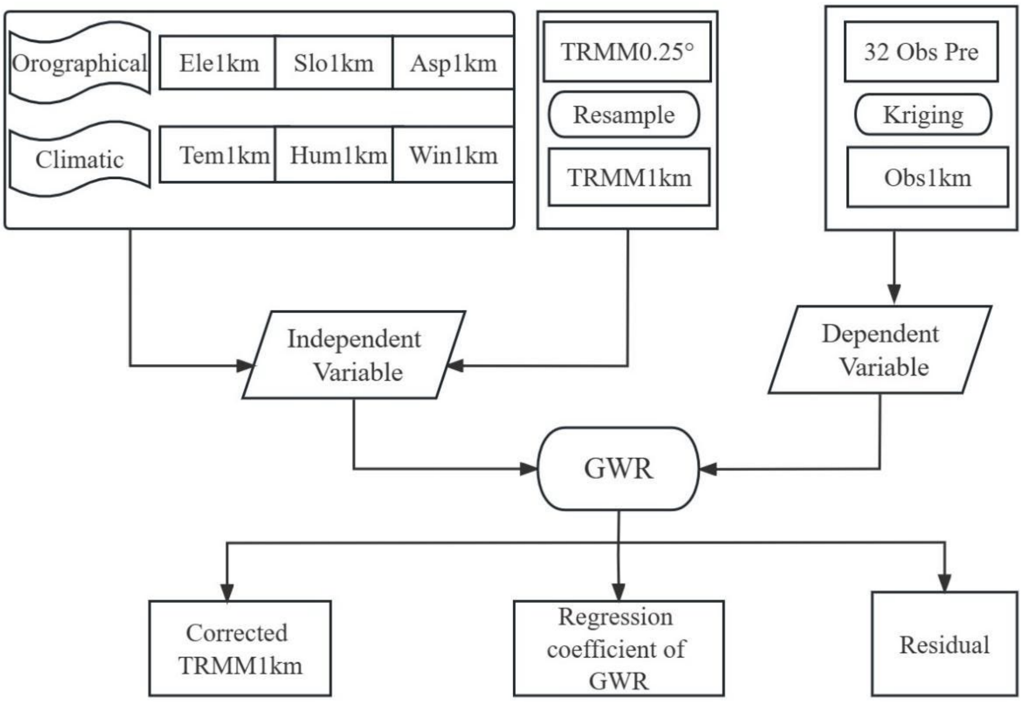

Fig.2 Flowchart of downscaling algorithm of GWR in this study

Table 1 Different models consider different parameters in GWR

Model	Parameters					
	Elevation	Aspect	Slope	Temperature	Wind speed	Humidity
1	✓					
2	✓	✓				
3	✓	✓	✓			
4	✓	✓	✓	✓		
5	✓	✓	✓	✓	✓	
6	✓	✓	✓	✓	✓	✓

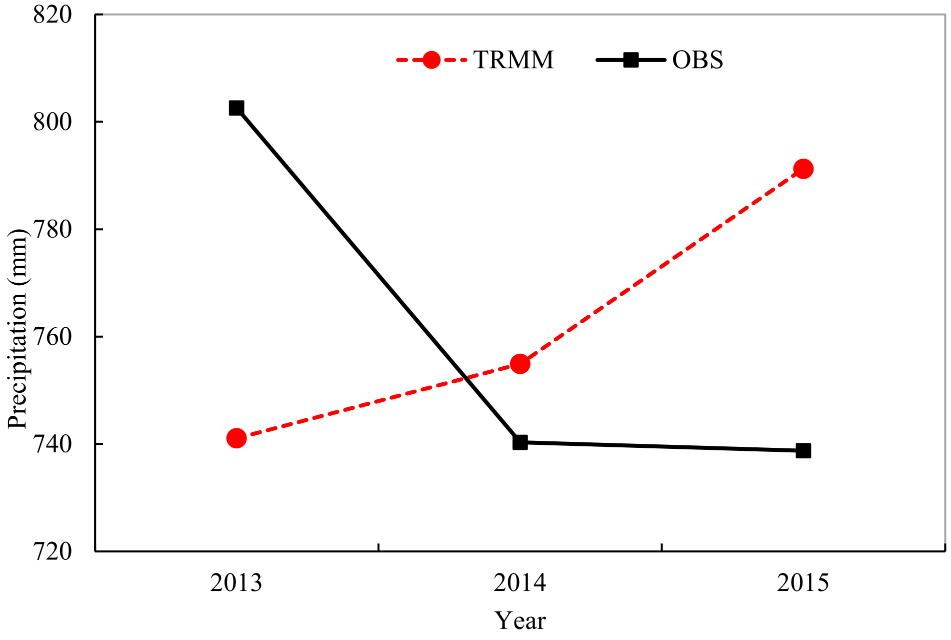

Fig.3 Comparison between the observed annual precipitation and annual TRMM 3B43 data during 2013 - 2015 periods in the Qinling Mountains

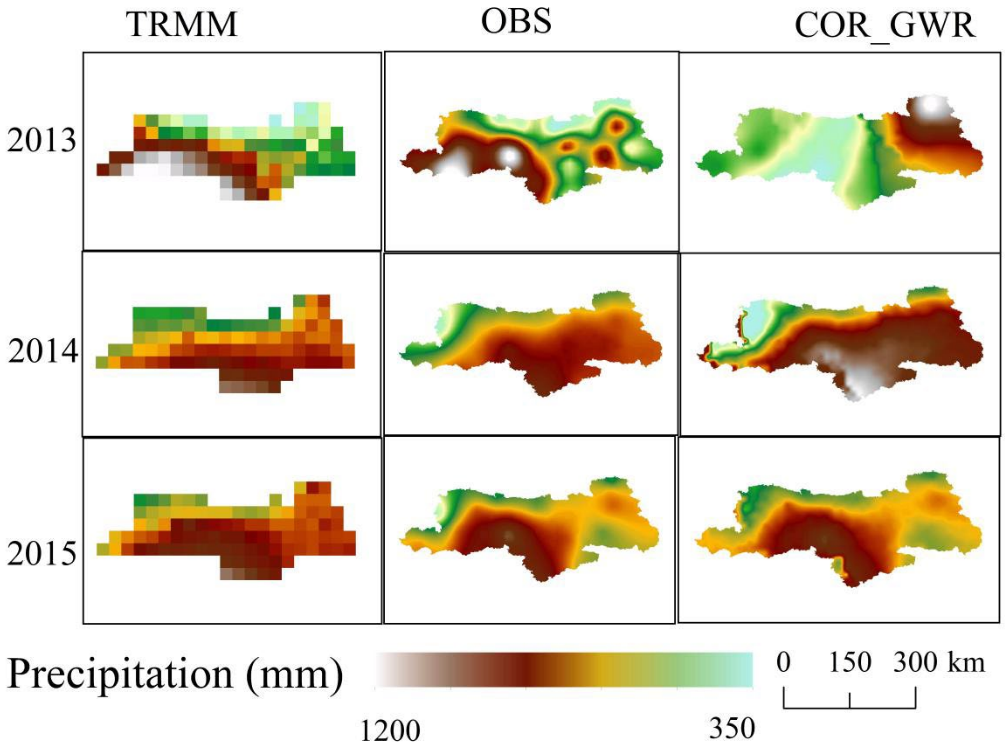

Fig.4 Spatial distribution of annual precipitation from 2013 - 2015 periods in the Qinling Mountains. The subscripts TRMM, OBS, and COR_GWR denote original TRMM data, interpolated observed precipitation data, and downscaled precipitation data by GWR.

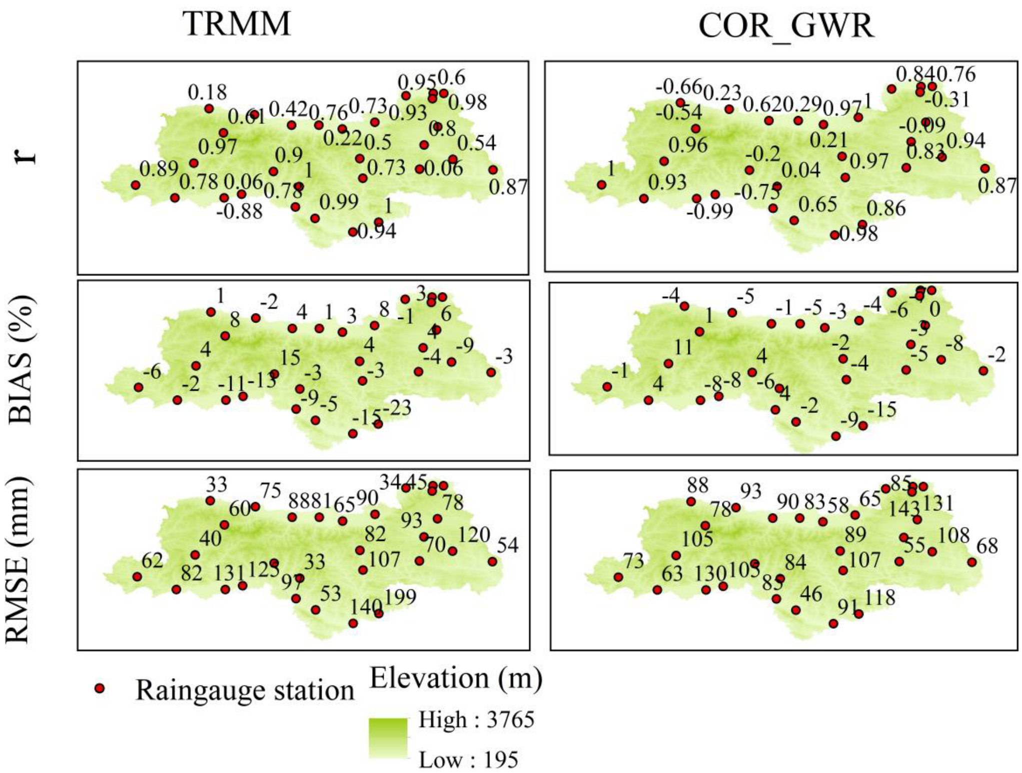

Fig.5 Spatial distribution of evaluation indices between original TRMM data and downscaled precipitation from 2013 - 2015 periods in the Qinling Mountains. The subscripts TRMM, and COR_GWR denote original TRMM data and downscaled precipitation data by GWR.

Table 2 Comparison between the observed precipitation and annual TRMM from 2013 to 2015 periods in the Qinling Mountains

Product	Year	Max (mm)	Min (mm)	Mean (mm)
TRMM	2013	1001.52	490.29	741.07
	2014	1020.74	560.81	754.95
	2015	1027.90	578.98	791.28
OBS	2013	1136.38	554.55	802.56
	2014	947.85	366.08	740.30
	2015	992.88	400.78	738.75
GWR	2013	1077.95	591.40	801.80
	2014	931.81	372.37	739.22
	2015	977.28	524.83	742.97

Table 3 Evaluation indices for annual TRMM and GWR from 2013 to 2015 periods in the Qinling Mountains.

Product	r	BIAS (%)	RMSE (mm)
TRMM	0.71	-3.60	99.31
GWR	0.86	-2.77	93.24

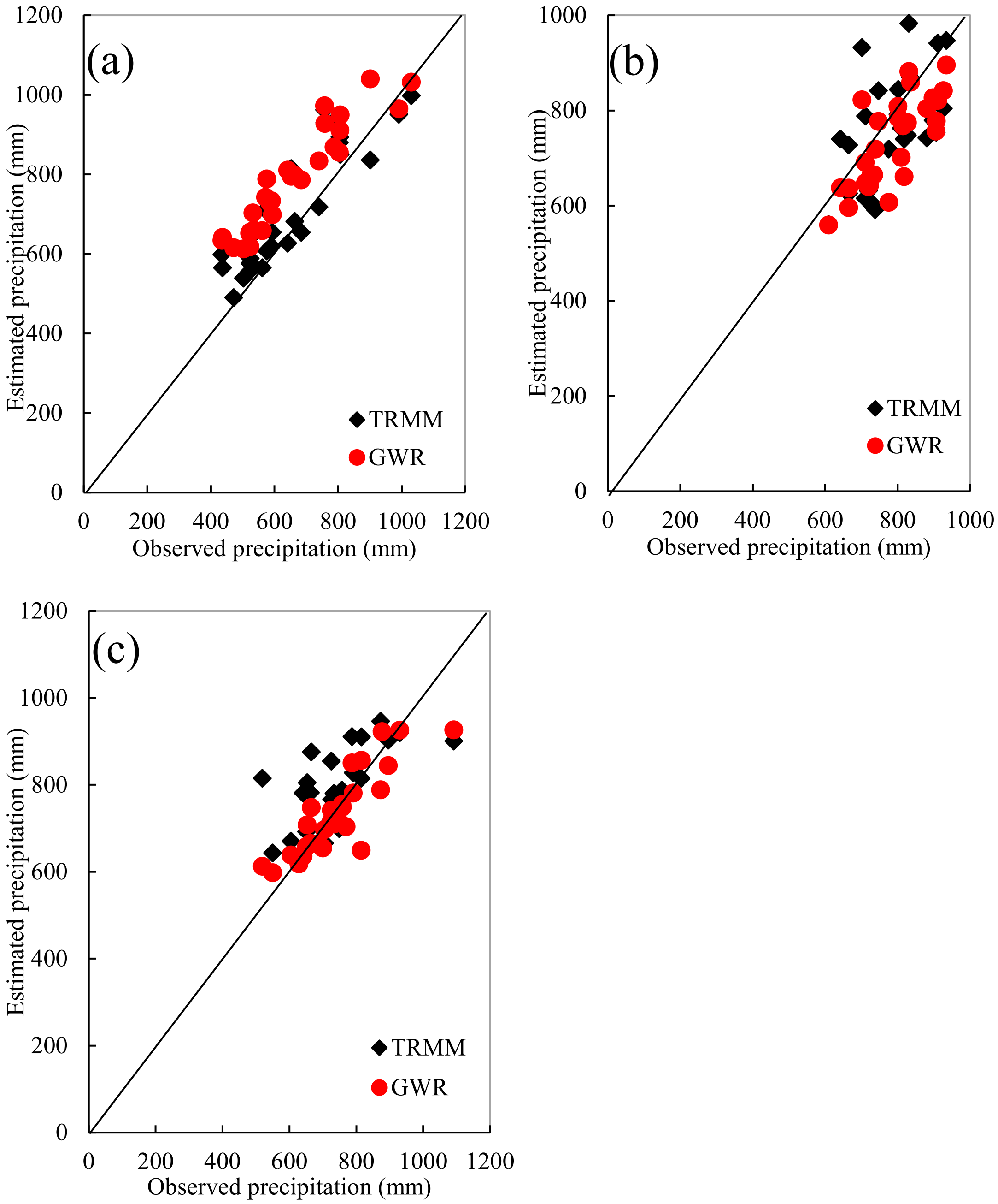

Fig.6 Scatter plots of annual TRMM and GWR model against the OBS.

(a) in 2013, (b) in 2014, and (c) in 2015.

Table 4 Comparison between different models of GWR from 2013 to 2015 periods in the Qinling Mountains

	r	BIAS (%)	RMSE (mm)
TRMM	0.71	-3.60	99.31
Model1	0.85	-3.23	94.05
Model2	0.85	-3.27	93.97
Model3	0.85	-3.27	93.84
Model4	0.85	-3.15	93.78
Model5	0.86	-2.93	93.41
Model6	0.86	-2.77	93.24

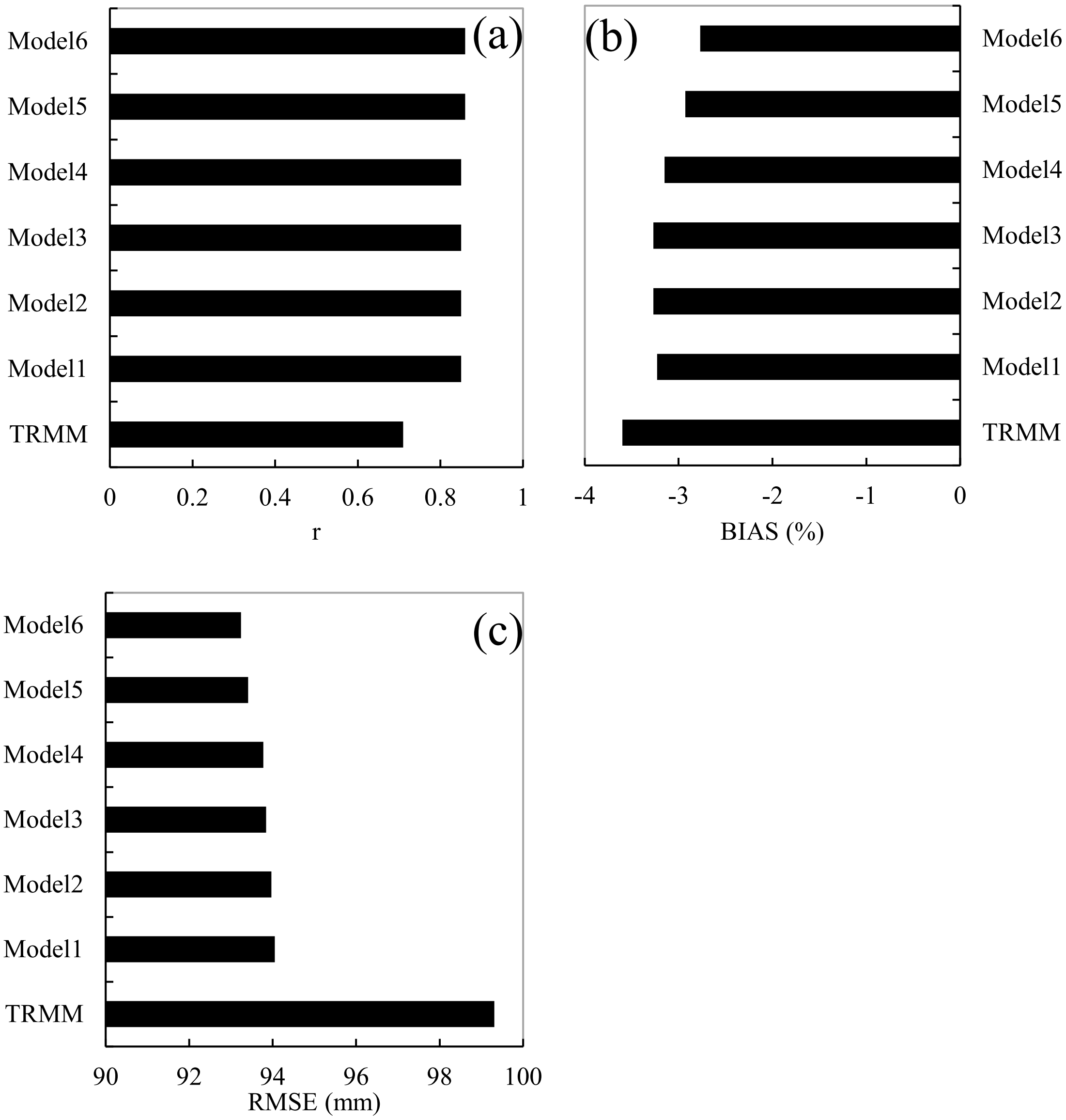

Fig.7 Bar plot of downscaled precipitation and TRMM data during 2013 - 2015 periods. (a) r, (b) BIAS, and (c) RMSE.

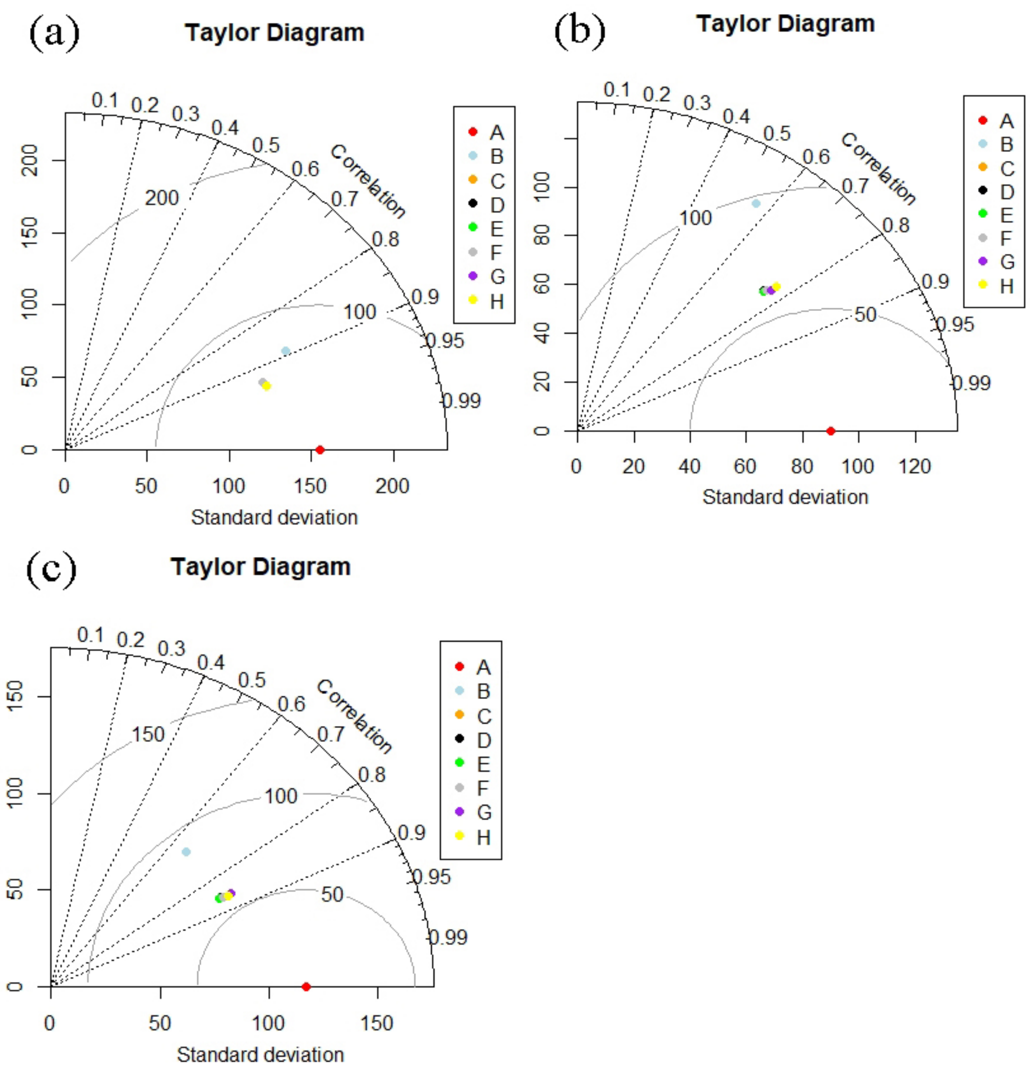

Fig.8 Taylor diagrams of different downscaled models with observed and TRMM. (a) - (c) denote in 2013, 2014, and 2015, respectively. Point A represents observed precipitation, and B represents TRMM data, C represents model 1, D - H represents model 2 - model 6, respectively.

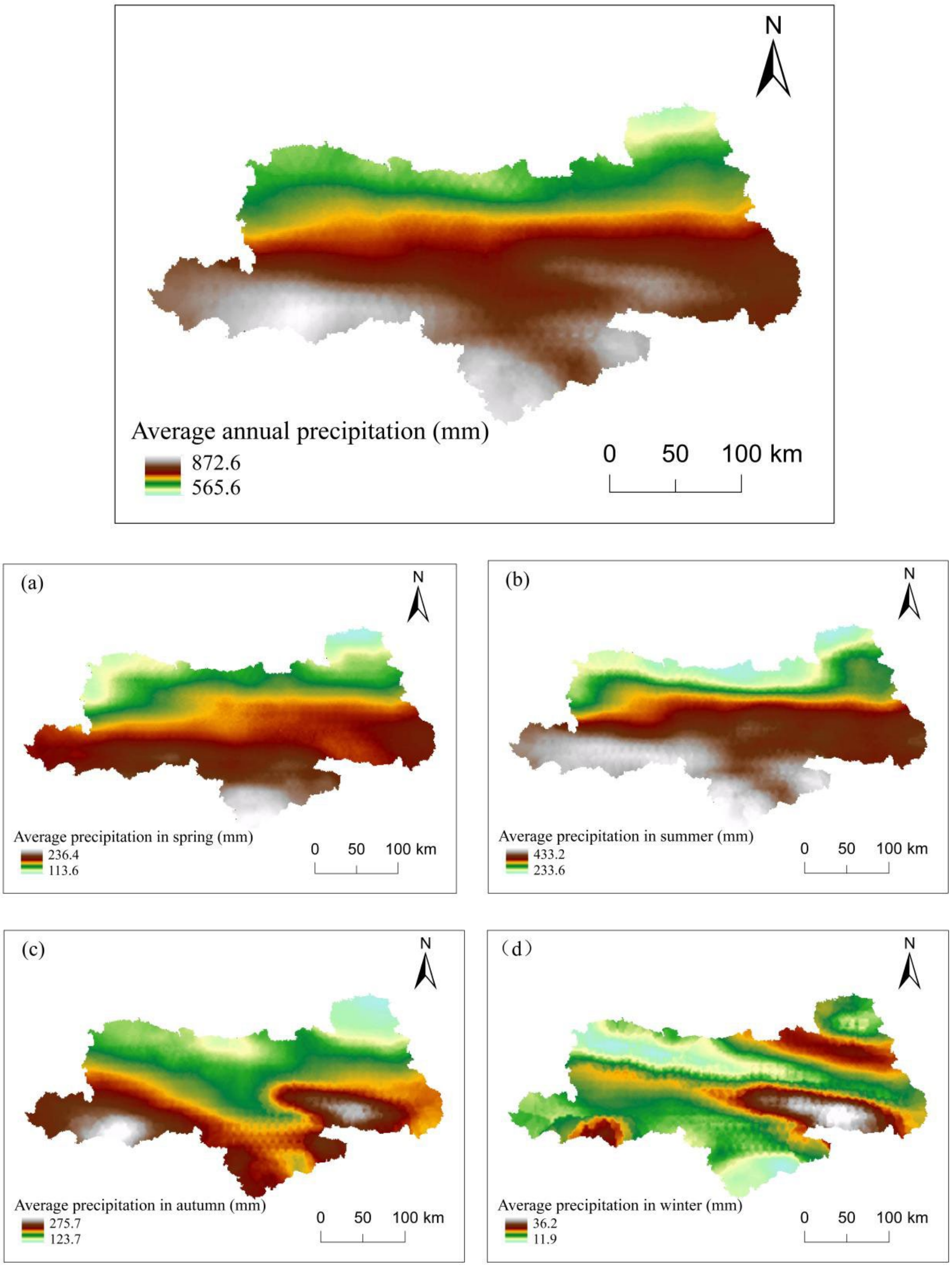

Fig. 9 Spatial Distribution of Annual and Seasonal Average Precipitation in the Qinling Mountains from 2002 to 2015 (a) Spring, (b) Summer, (c) Autumn, and (d) Winter

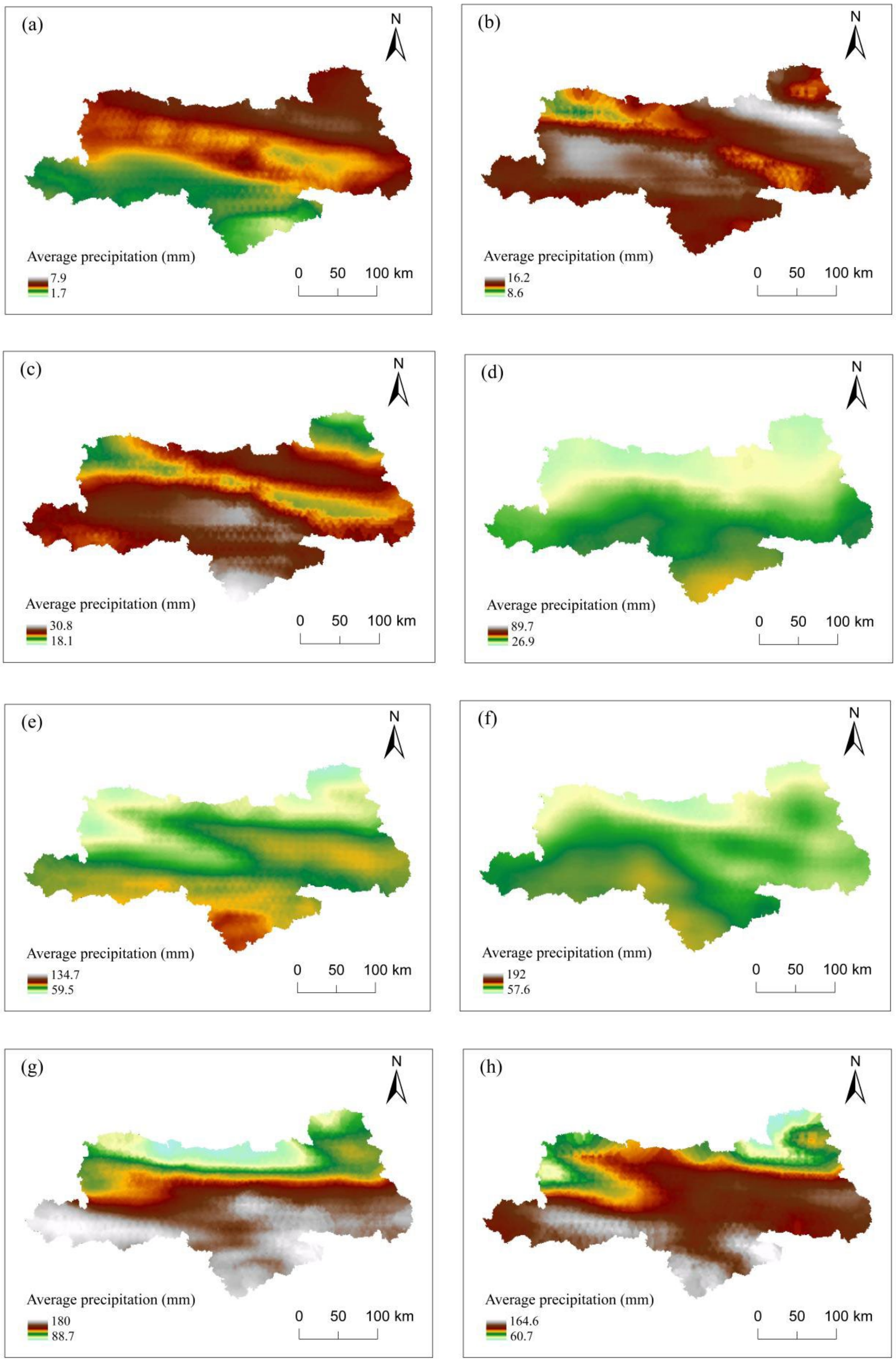

(a)
N
Average precipitation (mm)
7.9
1.7
0 50 100 km
(b)
N
Average precipitation (mm)
16.2
8.6
0 50 100 km
(c)
N
Average precipitation (mm)
30.8
18.1
0 50 100 km
(d)
N
Average precipitation (mm)
89.7
26.9
0 50 100 km
(e)
N
Average precipitation (mm)
134.7
59.5
0 50 100 km
(f)
N
Average precipitation (mm)
192
57.6
0 50 100 km
(g)
N
Average precipitation (mm)
180
88.7
0 50 100 km
(h)
N
Average precipitation (mm)
164.6
60.7
0 50 100 km

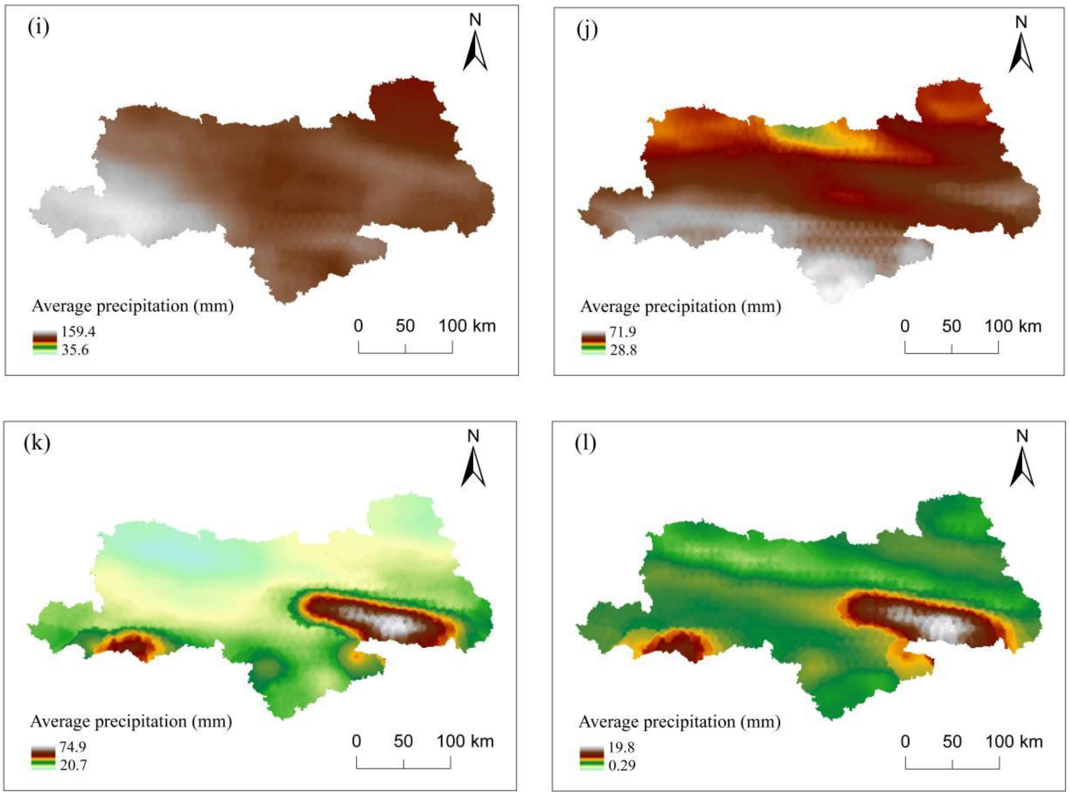

Fig. 10 Spatial distribution of monthly average precipitation in the Qinling Mountains from 2002 to 2015 (a) - (l) is from January to December, respectively

Table 5 Error testing of grid data sets of annual and seasonal average precipitation in the Qinling Mountains from 2002 to 2015

validation indices	Annual	Spring	Summer	Autumn	Winter
RMSE (mm)	78.24	19.05	39.87	31.60	6.66
r	0.79	0.85	0.83	0.59	0.17
BIAS (%)	-2.85	-7.94	1.65	-6.42	-0.97

Table 6 Error testing of monthly average precipitation grid dataset in the Qinling Mountains from 2002 to 2015

Validation indices	JAN	FEB	MAR	APR	MAY	JUN	JUL	AUG	SEP	OCT	NOV	DEC
RMSE (mm)	1.46	2.78	5.57	6.53	12.38	13.56	18.48	18.30	22.45	8.80	16.42	5.57
r	0.69	0.45	0.46	0.90	0.80	0.83	0.84	0.61	0.37	0.73	0.18	-0.03
BIAS (%)	-0.45	-0.26	1.07	-12.10	-8.38	8.67	-2.03	1.26	-9.76	-2.03	0.50	-2.85